Automated assessment of a kinetic database for fcc Co–Cr–Fe–Mn–Ni high entropy alloys

OPEN ACCESS
IOP Publishing
Modelling and Simulation in Materials Science and Engineering
Modelling Simul. Mater. Sci. Eng. **29** (2021) 055007 (22pp) https://doi.org/10.1088/1361-651X/abf62b

Automated assessment of a kinetic database for fcc Co–Cr–Fe–Mn–Ni high entropy alloys

Katrin Abrahams, Setareh Zomorodpoosh, Ahmadreza Riyahi Khorasgani, Irina Roslyakova*, Ingo Steinbach and Julia Kundin

ICAMS, Ruhr University Bochum, Universitätsstr. 15044801, Bochum, Germany

E-mail: irina.roslyakova@rub.de

Received 27 October 2020, revised 5 March 2021
Accepted for publication 8 April 2021
Published 20 May 2021

Abstract

The development of accurate kinetic databases by parametrizing the composition and temperature dependence of elemental atomic mobilities, is essential for correct multicomponent calculations and simulations. In this work the automated assessment procedure for the establishment of CALPHAD-type kinetic databases is proposed, including the storage of raw data and assessment results, automatic weighting of data, parameter selection and automated reassessments. This allows the establishment of reproducible up-to-date databases. The proposed software, written in python, is applied to the assessment of a kinetic database for the fcc Co–Cr–Fe–Mn–Ni high entropy alloy using only tracer diffusion data for a sharp separation of thermodynamic and kinetic data. The established database is valid for the whole composition range of the five-component high entropy alloy.

Keywords: atomic mobilities, automated assessments, CALPHAD databases, cross-validation

(Some figures may appear in colour only in the online journal)

1. Introduction

Diffusion, describing the transport of matter, either with or without thermodynamic driving forces in form of concentration or chemical potential gradients, is a key process in the life-

*Author to whom any correspondence should be addressed.

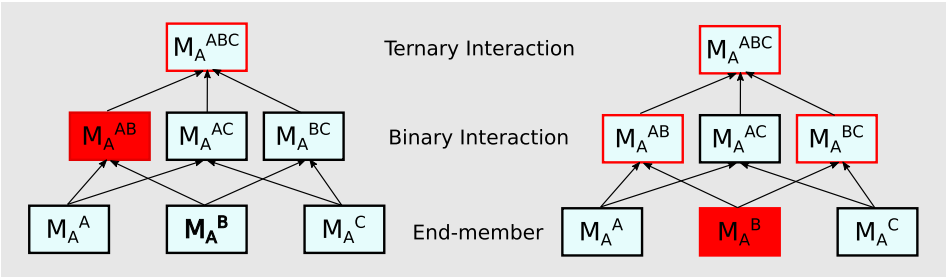

Figure 1. Dependencies of the assessed parameters in the different layers on each other and the reassessments that have to be conducted (marked with red boxes), if an end-member value, or a binary interaction term is rebuild. This is exemplified on diffusion of A in an A–B–C alloy [10].

time of a material [1–3]. Diffusion determines or influences for example phase transformation velocities [4], oxidation, annealing, pore formation and creep [5].

To predict and simulate correct diffusion behaviors, precise thermodynamic and kinetic descriptions of the investigated composition and temperature space are inevitable. Such data can be parametrized using the CALPHAD calculation of phase diagrams) method, which provides functional description for temperature and composition dependent models as well for the storage of the parameters in database (thermodynamics: so-called tdb-files (thermochemical database) and kinetics: so-called ddb-files (diffusivity database)) [6].

Thermodynamic databases, describing the Gibbs energies (unit: J mol^{-1}), exist for most of the important metallic material classes (e.g., Ni-based, Fe-based, or Al-based alloys). Kinetic databases contain parametrizations of the atomic mobility, defined as the velocity of a species per unit force (unit: m^2 s^{-1} J^{-1} mol) [7].

In the CALPHAD method, different models can be applied to describe the elemental distribution in phases, e.g., the sublattice model in the compound energy formalism (CEF) [6]. In the sublattice model, each phase is represented by one or more sublattices, where a set of equivalent positions, same Wyckoff positions, is treated as one sublattice. For simplicity, different sets of equivalent positions can be combined to one sublattice, but one set cannot be separated into several sublattices [6]. The sublattice description for face-centred cubic (fcc) Co–Cr–Fe–Mn–Ni is $(Co, Cr, Fe, Mn, Ni)_1(Va)_1$. Since it forms a solid solution, all positions are equivalent for the substitutional elements and the second lattice is only occupied by vacancies. To combine thermodynamic and kinetic databases the investigated phases must be represented with the same sublattice description.

The parametrization in the CALPHAD-technique is based on a pyramidal structure (see figure 1). The end-members, in thermodynamics the pure elements or stoichiometric compounds and in kinetics the diffusion in pure elements, form the basis. Dependent on these parameters additional interaction terms are added for accurate descriptions of alloying systems. Despite the advantages of straight-forward extrapolation to higher-order composition space, this assessment structure makes modifications cumbersome.

To overcome this problem ESPEI—extensible self-optimizing phase rquilibria infrastructure [8, 9] was developed for automated assessment of thermodynamic databases. A similar approach dealing with the automated assessment of atomic mobilities will be presented in this paper.

2. Modeling of CALPHAD-type kinetic databases

Atomic mobility databases contain models and the referring parameters to describe the composition, temperature, and pressure dependence of atomic mobilities. The functional form of the atomic mobilities are stored in so-called diffusion dataBases, DDB-files [11]. In the context of kinetic databases, it is important to clarify that the term *end-member* in the present work are pure elements Co, Cr, Fe, Mn, Ni. Note that for many phases modeled with the CEF the *end-members* cannot be pure elements and are diffusion species in a phase [12]. The term 'unaries' is misleading in case of atomic mobilities, since not only diffusion of A in A is an end-member but also the mobilities of all other elements in pure A. For example, in a binary A–B system, there are four end-members. In the following the mobility will be written as $M^{\text{Alloy}}_{\text{Diffusing Element}}$, e.g., A in pure A: M^A_A, A in pure B: M^B_A or A in A–B: M^{AB}_A. The main difference between thermodynamic and kinetic descriptions is that only one Gibbs energy exists for a phase, independent of the number of components. In contrast, n independent atomic mobilities exist in an n component alloy.

The temperature dependence of atomic mobilities can be described with the Arrhenius law (see equation (1)), since diffusion in solids occurs mainly via a vacancy-assisted process and the vacancy concentration is temperature dependent [13, 14]

$$M_i^k = M_i^{k,0} \exp\left(-\frac{Q_i^k}{RT}\right)\frac{1}{RT}, \tag{1}$$

where R (J mol^{-1} k^{-1}) is the ideal gas constant, T the temperature in Kelvin (K), $M_i^{k,0}$ the frequency factor and Q_i^k is the activation enthalpy (J mol^{-1}) for diffusion of i in k, where k stands for unary, binary, or higher order systems. This term can be extended for magnetic and ordering phenomena, which is described in detail in [14]. Q_i^k and $M_i^{k,0}$ can be grouped into one single parameter, $Q_i = -Q_i^k + RT\ \ln M_i^{k,0}$, in the case when there is no magnetic effect on the atomic mobility [13, 15]. It was found that $M_i^{k,0}$ is only slightly concentration dependent and thus the whole composition dependence is evaluated within Q_i^k [12, 16]. The Redlich–Kister expansion [17] plus ternary interactions give

$$\begin{aligned} Q_i = &\sum_{p=1}^{n} x_p Q_i^p + \sum_{p}^{n}\sum_{q>p}^{n} x_p x_q \left[\sum_{r=0}^{m} A_i^{pq,r}(x_p - x_q)^r\right] \\ &+ \sum_{p}\sum_{q>p}\sum_{v>q} x_p x_q x_v [v^s_{pqv} B_i^{pqv,s}]. \end{aligned} \tag{2}$$

The first term of equation (2) describes the interpolation between p end-members, and x_p, $p = 1, 2, \ldots, n$. The second term adds binary interaction terms x_p and x_q for the fitting parameter $A_i^{pq,r}$, where p and q, $q > p$, are the indexes of interacting elements and r is the order. The last term describes ternary interactions, following the symmetric thermodynamic approach with

$$\nu^s_{pqv} = x_s + \frac{(1 - x_p - x_q - x_v)}{3}, s \in (p, q, v) \tag{3}$$

and ternary interaction parameter $B_i^{pqv,s}$, which describes the influence of interactions between p, q and vth end-member on diffusion of element i.

The models are parametrized with the help of measured or calculated kinetic data. Mostly, tracer diffusion coefficients D_i, interdiffusion coefficients $\tilde{D}_{ij}$ and intrinsic diffusion coefficients ${}^iD_i$ are used. Tracer diffusion coefficients are directly related to atomic mobilities:

$D_i = M_i RT$, $i = 1, 2, \ldots, n$. Interdiffusion and intrinsic diffusion coefficients contain thermodynamic information and to extract atomic mobilities, assumptions about the thermodynamics are necessary. Thus such an extraction is ambiguous. The use of intrinsic and interdiffusion coefficients bounds the mobility database to the used thermodynamic databases, e.g., the mc_fe.tdb, release 2.060 database is linked to the mc_fe.ddb, release 2.012 [18]. This dependence is problematic if the thermodynamic database is, for example, updated of if someone wants to combine other databases. Note that in case of using the same CEF models and high-quality thermodynamic descriptions the same mobility database can be used with different thermodynamic databases [7].

The assessments procedure for kinetic databases follow a general procedure, consisting of the search for experimental data then the selection or weighting of these data, where the importance of each data-set is evaluated. In a next step, the end-member parameters are assessed and the number of binary and ternary interaction parameters is selected and those parameters are fitted to the data.

In literature, many mobility assessments are published, e.g., [7, 18, 19], but they have similar drawbacks:

- Addition of new data → the whole procedure has to be repeated, which is time-consuming.
- No general procedure for the weighting of data → person-dependent, not reproducible.
- No general procedure for the selection of parameters (model selection) → person-dependent, not reproducible.
- Atomic mobility assessments/databases are available for different parts of the phase diagram and, in general, cover the whole composition space. However, it is not clear how precise are the parameters for the extrapolation to areas where the experimental data do not exist yet. A universal automated approach for creating a mobility database covering the whole composition space and based only on the tracer diffusion data was not published previously.

To overcome these problems, a new standardized and automated assessment procedure is proposed in form of the automated assessment of atomic mobilities python-based software (PyMob) [10]. This framework handles the storage and weighting of raw data, model selection, assessment of model parameters, storage of assessed parameters and the reassessment procedures. To demonstrate the functionality of the proposed approach, we will apply this software to develop a purely kinetic database for fcc Co–Cr–Fe–Mn–Ni which is independent of all thermodynamic databases and valid for the whole composition range. It is worth to mention here that if the different thermodynamic descriptions to assess the self-diffusion mobilities are used, it becomes difficult to combine various binary and ternary assessments into large multicomponent systems. To efficiently develop a mobility database, one needs to create a self-consistent database that uses the same temperature and pressure functional descriptions of the mobility of pure elements. A similar problem was solved by Dinsdale [20] for CALPHAD multicomponent thermodynamic databases.

3. Automatisation

A new standardized and completely automated assessment procedure is proposed in form of the PyMob python-based software. This framework handles the storage and weighting of raw data, model selection, assessment of model parameters, storage of assessed parameters and reassessment procedures. The development of the PyMob software was inspired by the ESPEI—extensible self-optimizing phase equilibria infrastructure [8, 9] framework that

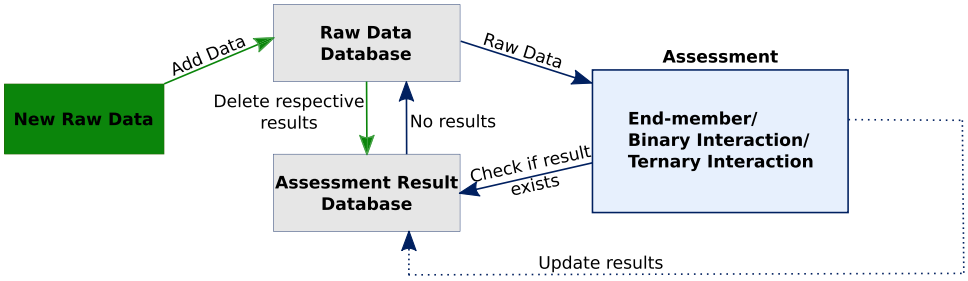

Figure 2. Software structure of PyMob [10].

deals with automated thermodynamic database development. This software will be available at ICAMS homepage [21]. In the following, first general software features will be presented and then the modified cross-validation approach [22, 23] and the parameter selection method are described in detail.

3.1. Technical details

The software written in Python (version 3.7) handles end-member assessments and the fitting of binary and ternary interaction terms. Due to the CALPHAD-type pyramidal structure, the binary interaction terms depend on the end-member results and the ternary interaction terms on the end-member and on the binary interaction terms. These three assessment stages are encapsulated and treated independently in the subsequent order. The assessment procedure on each stage is similar and shown in figure 2 with the blue circle. For every subsystem on the given stage, the following steps are executed: (1) check if the assessment result exists, (2) if yes, the assessment is not repeated and the next subsystem is chosen. If the result has not been already stored, the available raw data are collected, the assessment is conducted and the new results are stored and then the next subsystem is chosen for the assessment.

3.1.1. Data storage. Raw data, tracer diffusivities and Arrhenius parameters are tested against duplication and reasonability, and then they are stored in a structured query language (SQL) database. This allows automatic access and selection of the required data during an assessment step for the given sub-system. Thus, the user is not responsible for selecting the 'correct' data. In reverse conclusion it also means that not only user-selected data are used for the assessment. This handling additionally ensures that data are reusable in prospective assessments and it preserves resources, since the raw data do not have to be entered again, which also decreases the error rate.

The assessment results are also stored in SQL databases. This allows encapsulation of each assessment stage and fast accessing, e.g., to check if the results exist already and thus an assessment is not necessary for a given subsystem or to construct a ddb-file for further applications.

3.1.2. Fitting method. Taking the simplest case (no magnetic or ordering contribution), the temperature dependence of end-member data is fitted using Arrhenius law. For the elements which are ferromagnetic in fcc structure it is not valid. In particular, the problem of Curie temperature for Co was investigated in many works, e.g. [15]. We omit this effect in this paper and keep that for the future work. To estimate the best set of parameters for this model, the maximum likelihood estimation (MLE) can be used [24]. The likelihood function $\mathrm{L}(\theta_1, \ldots, \theta_p; X) = P(X|\Theta, M)$ is defined as the probability P of observing the data $X = (x_1, x_2, \ldots, x_n)$ using the

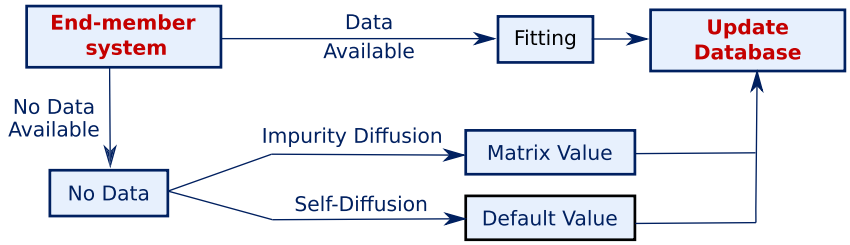

Figure 3. Dealing with lack of data in end-member assessments [10].

model M with the parameters space Θ. The observed data are, for example, outcomes of an experiment. The aim of MLE is to find the values of the model parameters that maximize the likelihood function over its parameter space

$$\hat{\theta} = \arg\max_{\theta\in\Theta} \widehat{L}(\theta\,; X) = \arg\max_{\theta\in\Theta} P(X|\Theta, M). \tag{4}$$

In our case the model M is the Arrhenius law from equation (1), where $\theta_1 = \frac{M_i^{k,0}}{RT}$ and $\theta_2 = Q_i^k$ are parameters to be estimated from data, R is gas constant and T is the temperature. In the *MLE* the parameters are determined such, that they maximize the likelihood that the Arrhenius model describes the observed experimental data. In this work, we assume that the tracer diffusion data has a normal (Gaussian) probability distribution, since the determined data are subject to a number of uncertainty sources, e.g., purity of the sample, temperature measurement, and the accuracy of the sectioning technique. These errors add up and the central limit theorem states that although the single uncertainty sources can have different distributions, their sum approaches the normal distribution [25]. On that condition the *MLE* can be technically implemented as the least squares method, which in general form can be defined as equation (5) (further details can be found in statistical textbooks, e.g., in [24])

$$\overrightarrow{\theta} = \arg\min_{\overrightarrow{\theta'}\in\Theta} \sum_{i=1}^{n} w_i(y_i - M(x_i, \overrightarrow{\theta'}))^2, \tag{5}$$

where Θ is parameter space, x_i is an independent variable, w_i is associated with the weight of ith data, and n is the number of data points. y_i and $M(x_i, \overrightarrow{\theta})$ are actual and estimated values of dependent variable, respectively. arg min returns a vector $\overrightarrow{\theta}$ for which $\sum_{i=1}^{n} w_i(y_i - M(x_i, \overrightarrow{\theta}))^2$ obtains its smallest value.

3.1.3. End-member assessment. The end-member assessment is special, since the parameters are critical. The procedure is shown in figure 3. If raw data are available, these data are assessed. If there are no data, it is distinguished between impurity, e.g. diffusion of A in B, and self-diffusion, e.g. diffusion of A in A. In case of impurity diffusion, the matrix value is adapted, meaning in this case the assessed parameters for B diffusion in B. For self-diffusion the frequency factor is chosen as 1×10^{-5} [26, 27] and the activation energy is calculated, using its relation to the melting point [28]. It can also be calculated with DFT data, e. g. self-diffusion coefficients of fcc Ni [29], but it is complicated and time-consuming.

3.1.4. Reassessment. In general, a reassessment is necessary if new raw data are added to the database. Therefore, due to the CALPHAD-type pyramidal structure shown in figure 1,

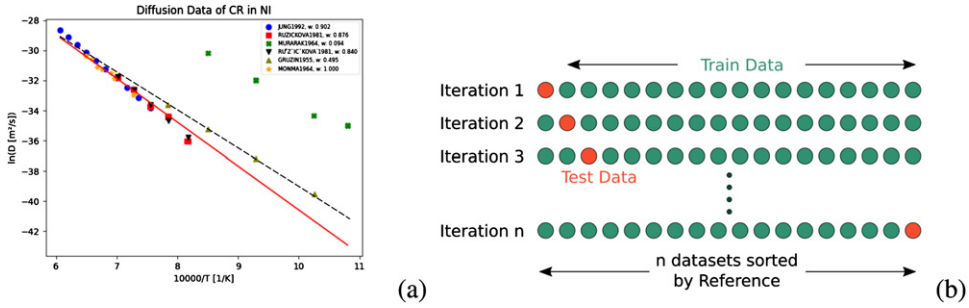

Figure 4. (a) Distribution of Cr diffusion data in pure Ni, measured by different research groups, and comparison between assessments with equally weighted data (dashed line) and with weighted data (solid line) using the modified CV method. (b) Iterative procedure for the split into test and train data in the CV approach [10].

multiple assessments results can be affected [30]. To ensure an update of all necessary parameters, the assessment results of all directly or indirectly concerned parameters are deleted from the assessment result database (compare the green part in figure 2). The assessment cycle is started automatically after the addition of raw data and the deleted assessment results will be replaced by the reassessed results.

3.2. Cross-validation

The previous works in the direction of the optimization of the estimation of the CALPHAD-based thermodynamic model parameters used the Markov Chain Monte Carlo technique with the criteria based on the classical Cramér–Rao bound [31–33]. A variety of raw data is stored in the database and they are often measured by different research groups, using samples of diverse purity and different laboratory equipment. For example, in figure 4(a), the tracer diffusion data for Ni in pure Ni are shown and colored for different references. It can be directly seen, that data-set 10 differs significantly from the other ones. The modified K-fold cross-validation (KFCV) method, which is proposed as a reproducible method to weight heat capacity data-sets automatically [22, 23] can be adapted and applied to tracer diffusion data. In original KFCV all data are split into k equal-sized data-sets (typically $k = 5$–10) randomly. Then, $k - 1$ data-sets form the training data that are used to evaluate the model parameters, and the left-out data-set, the test data-set, is used for testing. The distribution between train- and test-data is resampled such that every data-set is once used as a test data-set (see figure 4) [24]. In the modified KFCV method, in contrast to the original KFCV, each fold is chosen deliberately with a different size. As in the case of diffusion data, one can assume that the outlying data or the discrepancies between the data occur due to errors in the experimental set-up, e.g., purity of the sample or inaccuracy of experimental devices. Mostly one data-set, published by a research group, uses samples from the same source and conducts the experiments using the same experimental devices. Therefore, these data are assumed to have the same ‘experimental error’. To include this knowledge, the data are not split randomly into equal-sized sets (as it is provided in a general CV procedure), but instead, they are separated by reference, resulting in datasets of varying sizes. This provides the possibility to estimate the uncertainty of every single dataset from different references or available sources to be included in CALPHAD-type assessment. This is shown for Ni diffusion into Ni in figure 4, where the data from 16 different references are marked with diverse colors.

Table 1. Resulting assessment parameters for the weighted (with modified CV) and non-weighted (without modified CV) fit for Ni diffusion into Ni.

	Non-weighted	Weighted
$D_0(\mathrm{m^2\ s^{-1}})$	1.50×10^{-4}	1.00×10^{-5}
$Q(\mathrm{J\ mol^{-1}})$	204 675	241 220

The procedure to determine the weights of the different sets is as follows:

(a) Check if the data-set contains data from more than three references:
→ no: stop, not sufficient for CV,
→ yes: continue.

(b) Divide raw data by references into k data-sets.

(c) For every data-set t in k:

1 Assign data-set t as test data, as shown in figure 4(a).
2 Assign data-sets $k \backslash t$ as train data, as shown in figure 4(a).
3 Evaluate model parameters using the train data.
4 Calculate residual standard error (RSE) for the test defined as

$$\mathrm{RSE} = \sqrt{\frac{\sum_{i=1}^{n}(y_i - \hat{y}_i)^2}{n - p - 1}}, \tag{6}$$

where p is the number of model parameters, n is the number of data points, y_i and $\hat{y}_i$ are actual and estimated dependent variable, respectively.

(d) Determine $\mathrm{RSE_{min}}$ and $\mathrm{RSE_{max}}$.

(e) Calculate the weight for each data-set using the following equation

$$w_j = 1 - \frac{\mathrm{RSE}_j - \mathrm{RSE_{min}}}{\mathrm{RSE_{max}}} \tag{7}$$

for $j = 1, 2, \ldots, k$, where k is the number of data-sets.

The weights for the different data-sets for Ni diffusion into Ni are presented in figure 4(a). The CV method assigned a low weight to the outlying data-set 10. Here, the value of weight is in the range of [0, 1]. Using equation (7) automatically implies that the data-set with the lowest RSE obtains a weight of 1.0 and the distribution of weights depends on the difference between $\mathrm{RSE_{min}}$ and $\mathrm{RSE_{max}}$. For example, for Ni diffusion into Ni, data-set 10 obtains the lowest weight of 0.01. In figure 4(a), the final fit using the weights obtained from modified CV is shown in red and a non-weighted fit is shown in black. The influence of data-set 10 can be directly seen in the final results. The assessed parameters are listed in table 1. Using the weighted data, instead of the non-weighted ones, results in a lower value for the prefactor and the activation energy.

3.3. Parameter selection

The binary and ternary interaction terms adjust the composition dependence of atomic mobilities in binary and ternary systems and they are only added if necessary [6]. Therefore, one has to make sure to avoid under- and overfitting [24, 34]. In case of underfitting, the model

does not capture the structure of the data, because parameters or terms are missing that would appear in a correct model. The fit and the predictive performance of an underfitted model is poor. In case of overfitting, too many parameters are used that describe the train-data exactly, but their predictive behavior is lost.

The number of interaction parameters depends on the existing data and the assessed end-member results. If new data are added or end-member parameters are modified, the number of required interaction parameters for a good fit can vary. For an automatic model selection, penalized likelihood criteria [24, 34], or other models like minimum description length [24] or parametric bootstrap [24] can be used. Following the example of ESPEI, the corrected akaike information criteria (AICc), a penalized likelihood criterion was chosen [34, 35] which tends to be more accurate and allows to avoid the overparameterization especially for small samples:

$$\mathrm{AICc} = 2p + n\ \ln(\mathrm{RSS}(n)) + \frac{2p^2 + 2p}{(n - p - 1)}, \tag{8}$$

where p is the number of parameters and residual sum of squares (RSS) is RSS:

$$\mathrm{RSS} = \sum_{i=1}^{n} (y_i - \hat{y}_i)^2, \tag{9}$$

where y_i and $\hat{y}_i$ are actual and estimated dependent variable, respectively.

4. Application and results

In this work, the proposed automated assessment procedure is applied to the development of a database for fcc Co–Cr–Fe–Mn–Ni. As raw data only tracer diffusion data are used to ensure an independence of thermodynamic databases. The database, in the following referred to as *Tracer DB*, is valid for the whole composition range.

4.1. Available raw data

The available raw data are the basis for the assessment in the following sections. Tracer diffusion data are either available as single tracer diffusion coefficients (at one temperature and one composition), or in form of a parameterized Arrhenius law (prefactor and activation energy, see equation (1)), describing a temperature range. In the second case, single data points were re-calculated in equal distances for the given temperature range. Therefore, the same amount as initially measured data points is reconstructed, and if the number of data points is not available, it is assumed to be two, because this is the minimum for an Arrhenius fit. This results in total of 2222 data points for the fcc Co–Cr–Fe–Mn–Ni system: 578 data for Co diffusion, 268 data for Cr diffusion, 535 data for Fe diffusion, 116 data for Mn diffusion and 725 data for Ni diffusion. The available data for Co, Cr, Fe, Mn and Ni in end-member (blueish), binary (reddish) and ternary (greenish) sub-systems of Co–Cr–Fe–Mn–Ni are shown in figure 5. Diffusion data in pure Cr and Mn are not available since Cr does not form a stable fcc structure and fcc Mn is stable only in a small temperature interval. The amount and the distribution of available raw data differs strongly with the diffusing element, e.g. for Co and Mn there are no diffusion data in ternary alloys.

4.2. Assessment results

The assessment procedure has three steps and therefore the assessment results are split into the end-member results, binary interaction and ternary interaction terms. The uncertainty for

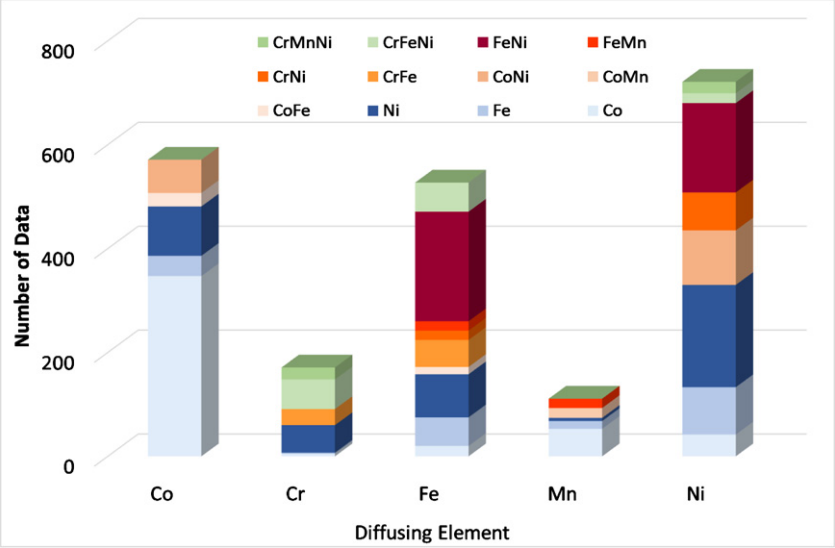

Figure 5. Available tracer diffusion data for Co, Cr, Fe, Mn and Ni in all unary (blueish), binary (reddish) and ternary (greenish) sub-systems of fcc Co–Cr–Fe–Mn–Ni [10].

Table 2. End-member assessment results for fcc Co–Cr–Fe–Mn–Ni systems.

Diffusing element	Matrix	M^0 (m^2 s^{-1})	Q(J mol^{-1})	Mode
Co	Co	1.50×10^{-4}	298158.15	Normal
	Cr	1.00×10^{-5}	308138.04	Adapted
	Fe	2.50×10^{-5}	283070.13	Normal
	Mn	1.00×10^{-5}	214713.62	Adapted
	Ni	1.29×10^{-5}	276224.19	Normal
	Co	8.40×10^{-6}	253700.00	Normal
	Cr	1.00×10^{-5}	308138.04	Default
Cr	Fe	3.32×10^{-3}	298611.12	Normal
	Mn	1.00×10^{-5}	214713.62	Adapted
	Ni	1.00×10^{-5}	241220.69	Normal
	Co	3.00×10^{-6}	237747.76	Normal
	Cr	1.00×10^{-5}	308138.04	Adapted
Fe	Fe	5.70×10^{-5}	280201.30	Normal
	Mn	1.00×10^{-5}	214713.62	Adapted
	Ni	5.60×10^{-5}	262050.02	Normal
	Co	6.00×10^{-6}	238061.23	Normal
	Cr	1.00×10^{-5}	308138.04	Adapted
Mn	Fe	3.00×10^{-6}	245525.98	Normal
	Mn	1.00×10^{-5}	214713.62	Default
	Ni	7.50×10^{-4}	280900.00	Normal
	Co	5.30×10^{-5}	281527.44	Normal
	Cr	1.00×10^{-5}	308138.04	Adapted
Ni	Fe	1.00×10^{-6}	230448.95	Normal
	Mn	1.00×10^{-5}	214713.62	Adapted
	Ni	8.90×10^{-5}	276666.70	Normal

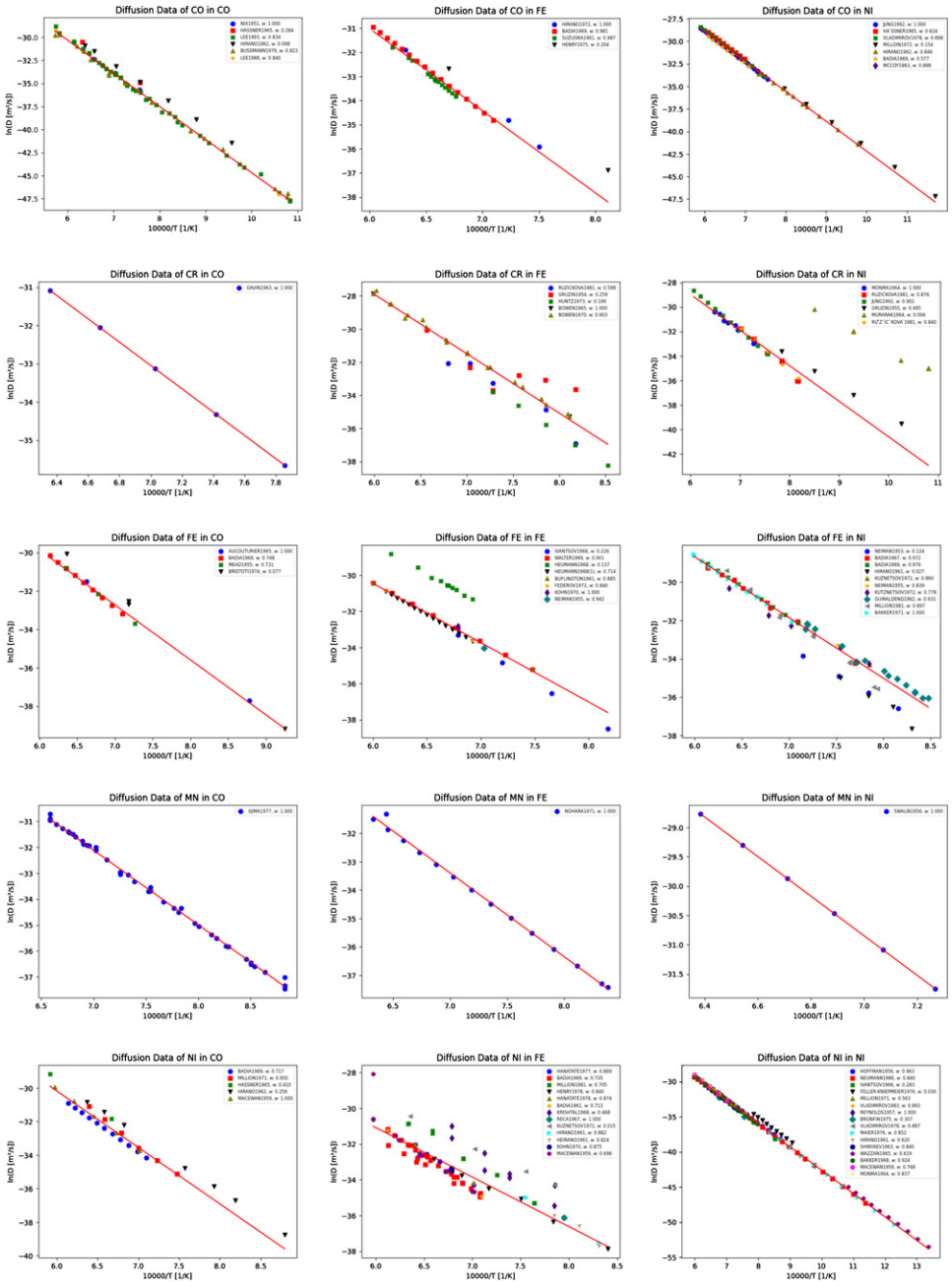

Figure 6. End-member assessment results for diffusion of Co, Cr, Fe, Mn, and Ni in fcc Co, Fe, and Ni.

the end-member model parameters was for the prefactor 5–50%, for the activation energy 0.25–5%, for binary parameters $>70\%$ according to reports of the fitting procedure.

Table 3. Comparison of the selected binary interaction terms using AIC criterion in fcc Co–Cr–Fe–Mn–Ni. An 'x' marks parameters that were not selected and lightblue colored boxes indicate acceptance. The numbers give the orders of the accepted parameters (see equation (2)).

	Diffusing Element				
Interaction	Co	Cr	Fe	Mn	Ni
Co–Cr	x	x	x	x	x
Co–Fe	1	x	2	x	x
Co–Mn	x	x	x	1	x
Co–Ni	1	x	x	x	2
Cr–Fe	x	0	2	x	0
Cr–Mn	x	x	x	x	0
Cr–Ni	x	2	1	x	2
Fe–Mn	x	x	x	2	0
Fe–Ni	x	2	2	x	2
Mn–Ni	x	0	x	x	x

4.2.1. End-member results. The end-member assessment results following equation (1) are listed for considered elements: Co, Cr, Fe, Mn, and Ni in table 2, which contains five columns: diffusing element, matrix, M^0, Q, and mode. The column **mode** indicates if raw data were available and a *normal* assessment was conducted, or if the data were *adapted* or *default* values were used (according to the scheme of end-member assessment presented in section 3.1.3). In figure 6, the end-member assessment results are presented. The results are obtained for diffusion in Co, Fe, and Ni, since data were available for these systems. The plots show the experimental tracer diffusion data in comparison to the calculated Arrhenius dependency with the fitting parameters from table 2. The experimental data are splitted by references and the corresponding weights calculated by CV method (section 3.2) are added for each reference for the information.

4.2.2. Interaction parameters. If the end-member assessments do not represent the composition dependence of the mobility data well, binary and ternary interaction terms can be added (according to Redlich–Kister equation (2)). To avoid overfitting, additional interaction parameters are selected using the penalized likelihood criterion AIC (see section 3.3 for more details).

The comparison between the selected parameters using the AIC criteria is shown in table 3 for the binary interaction terms. The fields marked by an 'x' indicate that the interaction parameter was not selected in the assessment process using the given criterion. A blue colored cell, states that the interaction parameter is chosen. In case of binary interaction terms, all possible interactions are listed and if a parameter is selected, also the order (see second term in equation (2)) of the parameter(s) is/are given.

4.2.2.1. Binary Interaction Parameters Binary interaction terms have an additional order term (r), the range can be from 0 to basically infinite. For binary systems in fcc Co–Cr–Fe–Mn–Ni, the interaction terms of order 0,1 and 2 were considered in the fitting procedure. The found parameters are listed in table 4. For binary systems that are not listed were either no diffusion data available, or additional interaction parameters are not necessary.

For Co diffusion, binary interaction terms are added for the Co–Fe and Co–Ni system. For Cr, parameters of 0th and 1st order are selected for the Cr–Ni and Fe–Ni system. Most interaction parameters are added for Fe diffusion. Not only in Fe binary systems (Fe–Co, Fe–Cr,

Table 4. Binary interaction parameters, determined using AIC (see equation (8)), for the fcc Co–Cr–Fe–Mn–Ni system.

Diffusing Element	Interaction	Order	Value
Co	Co–Fe	0	47774.39
Co	Co–Ni	0	39544.30
Co	Co–Ni	1	−17254.22
Cr	Cr–Ni	0	90989.25
Cr	Cr–Ni	1	76435.80
Cr	Cr–Fe	0	−104527.60
Cr	Fe–Ni	0	−21344.70
Cr	Fe–Ni	1	−29239.77
Fe	Fe–Co	0	−5426.16
Fe	Fe–Co	1	86414.68
Fe	Fe–Cr	0	−248776.44
Fe	Fe–Mn	0	3232919.08
Fe	Fe–Mn	1	−1582992.04
Fe	Fe–Ni	0	25886.58
Fe	Cr–Ni	0	−266605.63
Mn	Mn–Co	0	57901.61
Ni	Ni–Co	0	22873.17
Ni	Ni–Cr	0	−612586.00
Ni	Ni–Cr	1	581465.47
Ni	Ni–Fe	0	60435.86
Ni	Ni–Fe	1	−24352.99

Fe–Mn, and Fe–Ni), but also as impurity in the Cr–Ni system. For Mn, only one parameter is added for the Mn–Co interaction, and for Ni, additional parameters of 0th and 1st order are selected for the Ni–Co, Ni–Cr, and Ni–Fe system.

In figure 7, the composition (left figure) and temperature (right figure) dependent profiles for Fe–Co system are shown. The different colors indicate different temperatures (left figure), or rather different compositions (right figure). The composition dependence is described with a wave-like profile, reproducing the experimental data points well. In the right figure it can be seen that the predicted mobilities fit very good for 10 and 50 at.% Fe, while for 6 at.% Fe, the mobilities from *Tracer DB* deviate slightly from the measured data.

The composition and temperature dependence of Ni diffusion in Co–Ni is shown in figure 8. The amount of available experimental data is significantly larger than for the Co–Fe system. Again, during the assessment, parameters of 0th and 1st order were added, but with smaller parameter values than for Fe diffusion in Co–Fe, resulting in a slightly curved profile describing the composition dependence (see figure 8 left). The temperature dependent plot (see figure 8 right) reveals, that the higher the Ni concentration the better the agreement between *Tracer DB* and experimental data.

4.2.2.2. Ternary Interaction Parameters For ternary interactions, only parameters in the Cr–Fe–Ni system were evaluated, if it is needed by AICc, due to otherwise lack of data for other ternary system. The parameters that were automatically chosen using the PyMob software are given in table 5. For the ternary interaction parameters, there is no order, but instead a main element s is always provided (see equation (3)). For Cr diffusion in Cr–Fe–Ni, two parameters are added (for Cr and Fe as main element). For Fe diffusion, only two parameters,

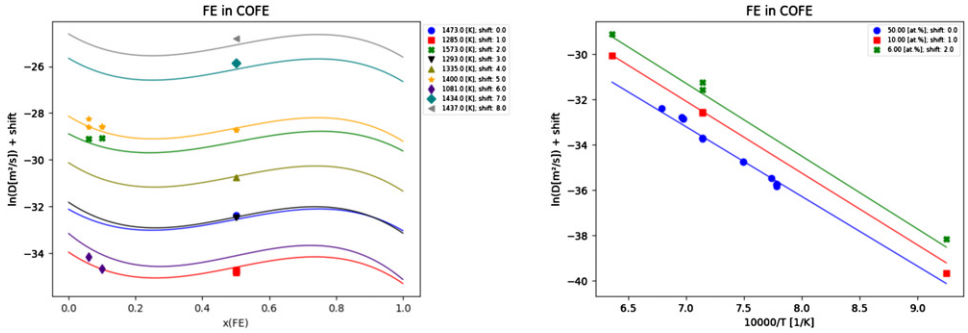

Figure 7. Comparison between the predicted mobilities from Tracer DB and experimentally measured data for Fe diffusion in Co–Fe. Left: composition dependence of ln(D), separated by temperature. Right: temperature dependence of ln(D), separated by composition.

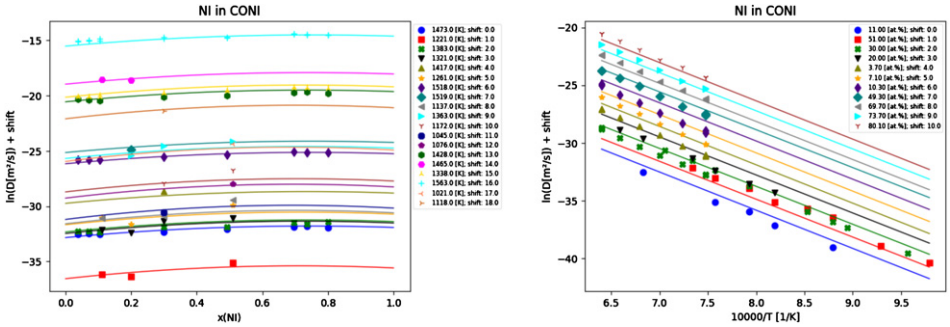

Figure 8. Comparison between the predicted mobilities from Tracer DB and experimentally measured data for Ni diffusion in Co–Ni. Left: composition dependence of ln(D), separated by temperature. Right: temperature dependence of ln(D), separated by composition.

Table 5. Ternary interaction parameters, determined using AICc (see equation (8)), for the fcc Co–Cr–Fe–Mn–Ni system. s refers to the element used in equation (3).

Diffusing element	Interaction	s	Value
Cr	Cr–Fe–Ni	Cr	672683.36
Cr	Cr–Fe–Ni	Fe	635353.79
Fe	Cr–Fe–Ni	Cr	−5198738.43
Fe	Cr–Fe–Ni	Ni	2257776.98
Ni	Cr–Fe–Ni	Fe	−4679404.54
Ni	Cr–Fe–Ni	Ni	2295218.52

for Cr and Ni as main elements, are chosen and for Ni diffusion two parameter, for Fe and Ni as main element, are selected.

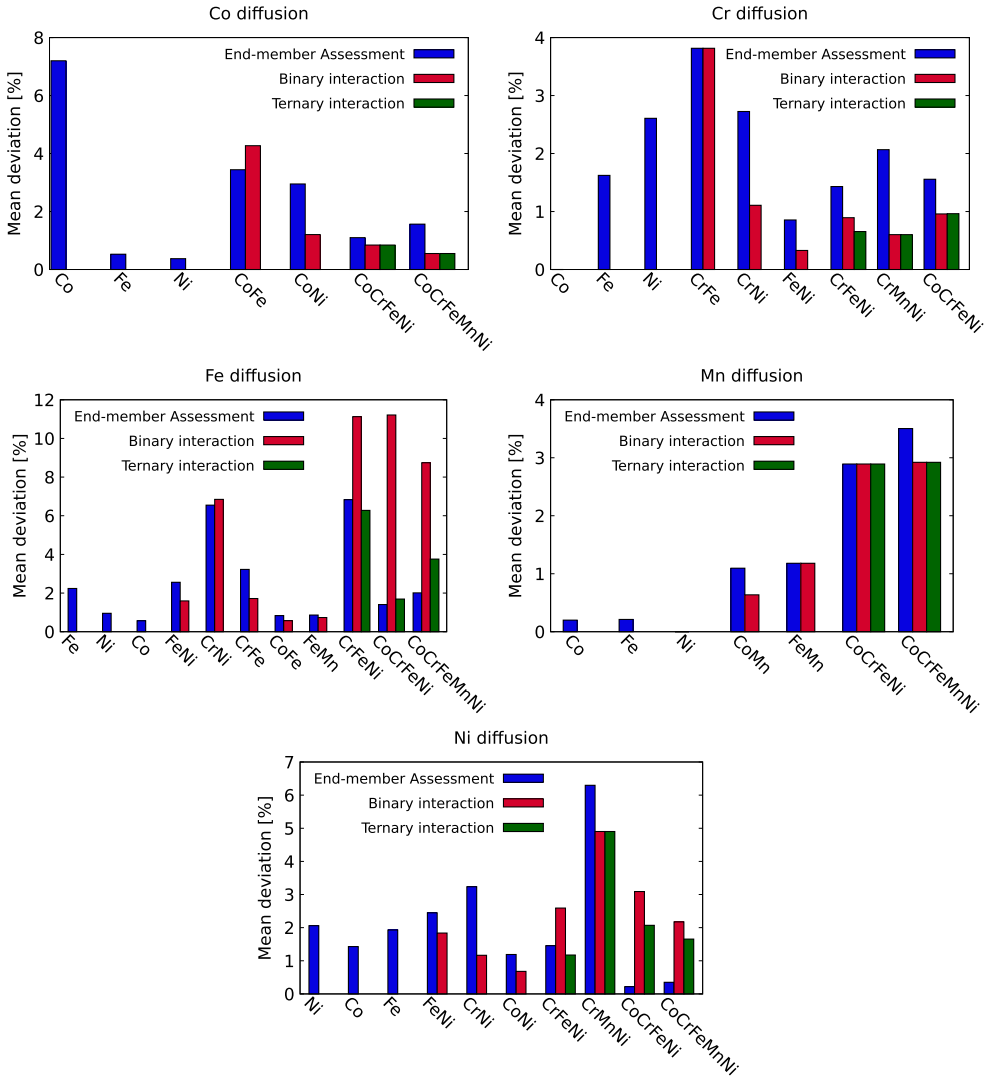

Figure 9. Influence of the addition of binary and ternary interaction parameters on the mean deviation of the assessment results from the measured data. The mean is always taken over one alloy system [10].

4.3. Influence of binary and ternary interaction terms

The influence of the addition of binary and ternary interaction parameters is summarized in figure 9. For every diffusing element, the mean deviation between the experimentally measured and predicted mobility/tracer diffusion coefficient is shown separately for every alloy. The deviation was calculated for every data point and then the mean was taken with respect to every sub-system. This was performed for three different scenarios: (1) only end-member assessment results are used to predict the mobilities (denoted as 'end-member assessment'), (2) binary interaction parameters are included (denoted as 'binary interaction'), and (3) the mobilities are predicted using end-member parameters, binary and ternary interaction terms

(denoted as 'ternary interaction'). For diffusion into one-component alloys (pure Co, Fe, or Ni) only the end-member results are presented, since binary and ternary interactions do not influence these results. The same accounts for ternary interaction parameters in binary alloys. For all higher-order systems, all three possibilities are revealed. The binary interaction term for Co diffusion in Co–Fe rises the mean deviation slightly, because here the mean deviation is calculated, while for the parameter selection (AICc) the RSS is used (see equation (8)), which punishes large deviations stronger. For Co diffusion into Co–Ni, Co–Cr–Fe–Ni, and Co–Cr–Fe–Mn–Ni the binary interaction term lowers the mean error significantly. The results including ternary parameters do not change, since no ternary parameters were selected during the assessment for these systems. Concerning Cr diffusion, the binary interaction term lowers the mean deviation for all binary systems, except for Cr–Fe where no parameter was chosen, and all higher-order systems significantly. Also ternary interaction terms were parametrized and led to further improvement. In case of Fe diffusion, the binary interaction terms increase the mean deviation in ternary and higher-order systems. The addition of ternary interaction parameters decreases in general the mean deviation. However, the parameters for Fe–Cr interaction are strongly biased in such a sense that the raw data only represent Fe-rich or Cr-rich part of the phase-diagram, this influences the results for four- and five component alloys. The lack of data for Mn diffusion results in only one binary interaction parameter for Co–Mn, but this influences the results for higher-order data positively. For Ni diffusion, all three binary interaction terms in Cr–Ni, Co–Ni, and Fe–Ni decrease the mean deviation in the binary systems and in the Cr–Mn–Ni system, but increase it in Cr–Fe–Ni. The addition of a ternary interaction parameter for the Cr–Fe–Ni system decreases the deviation again. Interestingly, in case of Ni diffusion in Co–Cr–Fe–Ni and Co–Cr–Fe–Mn–Ni, the best results are obtained with only using the end-member assessment results. The diffusion data in the Co–Cr–Fe–Mn–Ni and Co–Cr–Fe–Ni system were not taken into account in this assessment. Here, they are used to test the extrapolation to four and five component systems. For Co, Cr, and Ni diffusion, the mean deviation in both systems is around 1%, and for Fe and Mn around 3%, which is smaller than the experimental accuracy [36].

5. Conclusions

A software for automated assessment and reassessment of atomic mobilities was developed with the following advantages over conventional assessments:

- **Automatic storage of raw data in SQL databases.** It is ensured that not only selected data are used, but all available data. Additional data can be easily added and during a reassessment old and new data are employed.
- **Automatic administration of assessment results.** The assessed results are stored in SQL databases for easy access and reuse. Due to automatic reassessment, these parameters are always up-to-date.
- **Automatic weighting of data.** A modified CV method was implemented, to weight the data from different references with respect to each other. Due to the rare number of tracer diffusion data, a separation of data into pure test and train data is not reasonable.
- **Automatic selection of interaction parameters.** Since the number of binary and ternary interaction parameters depends on the end-member assessments, the alloy, and the experimental data, the selection is automatized. To avoid overfitting, a penalized likelihood criterion is chosen: corrected AICc.
- **Automatic reassessment.** If new raw data are added, one or several parameters have to be reassessed. These parameters are automatically tagged and a reassessment is initiated.

- **Reproducible results:** since all steps are automatized, the assessment is independent of the user and can be repeated.

The automated assessment software PyMob was applied to develop *Tracer DB*, a universal database, purely based on tracer diffusion data. Other data, like interdiffusion or intrinsic diffusion coefficients were not included. Although this reduces the amount of usable data, a purely kinetic database could be established. Interdiffusion and intrinsic diffusion data consist of a thermodynamic and a kinetic part and to extract only the kinetics, a thermodynamic database or other thermodynamic values have to be used. This bounds the kinetic database to the chosen thermodynamic database, which is avoided for Tracer DB. Furthermore, Tracer DB is valid for the whole composition range and not only for a specified part of the phase diagram, as it is the case for conventional databases.

These preliminary requirements were applied to the development of an atomic mobility database for the fcc Co–Cr–Fe–Mn–Ni system (see section 4.2.2). This system was chosen due to its challenging elements, such as Cr and Mn, that do not form a stable fcc structure. Furthermore, many experimental tracer diffusion data were found in literature, not only for the pure elements and binary system, but also for higher-order systems, even for the equiatomic five-component alloy. The assessment included binary and ternary interaction parameters, but the four- or five-component data were not used in the assessment. Therefore, these data could be utilized to verify and check the extrapolation to higher-order data. Data for end-member assessments were available for diffusion of Co, Cr, Fe, Mn, and Ni in Co, Fe, and Ni (see section 4.1). Especially for Co and Ni self-diffusion, outlying data-sets were found, which were lowly weighted by the CV method (see section 3.1.3). Several binary and even ternary interaction terms were added (see section 4.2.2). It was found that the average deviations in the four and five component alloys were below 8 %. For Co, Cr, and Ni diffusion the deviation was even below 2%.

Acknowledgments

We would like to thank Deutsche Forschungsgemeinschaft (DFG) for the financial support under the research contract STE 116/30-2 and SFB TR-103, Project T2.

Data availability statement

The data generated and/or analysed during the current study are not publicly available for legal/ethical reasons but are available from the corresponding author on reasonable request.

Appendix. Abbreviations of the references used in PyMob

For the assessment of the diffusion data many experimental data were collected. Some were taken from previous assessments, e.g. from [37–40]. Others were taken either from their original paper or taken from books (e.g. [36, 41]). For a correct allocation, here we refer to the original reference. If the original reference was not available, the corresponding book, where the data are taken from, is cited. In the figures, obtained from PyMob, the references are given by 'last name of first author + year' for simplicity. The relation to the citation used in this paper are given in table 6.

Table 6. Relation between the reference scheme implemented in PyMob, and therefore, also used in graphs obtained from PyMob, and the reference scheme used in this work.

Reference in PyMob	Reference this Work	Reference in PyMob	Reference this Work
Aucouturier1965	[42]	Krishtal1968	[43]
Badia1961	[41]	Kuznetsov1972	[44]
Badia1967	[45]	Lee1988	[46]
Badia1969	[47]	Lee1993	[48]
Bakker1968	[49]	MacEwan1959	[50]
Bowen1965	[41]	Maier1976	[51]
Bowen1970	[52]	Mead1955	[53]
Bristoti1974	[54]	Million1969	[55]
Bronfin1975	[56]	Million1971	[57]
Buffington1961	[58]	Million1972	[59]
Bussmann1979	[60]	Million1985	[61]
Davin1963	[62]	McCoy1963	[63]
Duhaunay1979	[41]	Monma1964	[64]
Fedorov1963	[65]	Murarak1964	[66]
Fishman1970	[41]	Neimann1953	[67]
Gaertner2018	[68]	Neimann1955	[69]
Gruzin1954	[70]	Neumann1986	[71]
Gruzin1955	[72]	Neumann2001	[73]
Guiraldenq1962	[74]	Nix1951	[75]
Haessner1965	[76]	Nohara1970	[77]
Henry1975	[78]	Nohara1971	[79]
Henry1978	[80]	Nohara1973	[81]
Heumann1986	[82]	Reca1967	[83]
Hirano1962	[84]	Rothman1980	[85]
Hirano1972	[86]	Ruzickova1970	[87]
Hoffmann1956	[88]	Ruzickova1981	[87]
Huntz1973	[89]	Shinyaev1963	[90]
Iijima1977	[91]	Suzuoka1961	[92]
Ivantsov1966	[93]	Swalin1956	[94]
Jung1992	[95]	Vladimirov1978	[96]
Kohn1970	[97]	Wazzan1965	[98]

ORCID iDs

Setareh Zomorodpoosh https://orcid.org/0000-0002-9198-6156
Irina Roslyakova https://orcid.org/0000-0003-4329-6502
Ingo Steinbach https://orcid.org/0000-0002-2834-1160
Julia Kundin https://orcid.org/0000-0003-0181-8130

References

[1] Mehrer H 2007 *Diffusion in Solids: Fundamentals, Methods, Materials, Diffusion-Controlled Processes* (*Springer Series in Solid-State Sciences*) (Berlin: Springer)
[2] Gupta D 2005 *Diffusion Processes in Advanced Technological Materials* (Norwich, NY: William Andrew Publishing)
[3] Paul A, Laurila T, Vuorinen V and Divinski S V 2014 *Thermodynamics, Diffusion and the Kirkendall Effect in Solids* 1st edn (Berlin: Springer)
[4] Inden G and Neumann P 1996 Simulation of diffusion controlled phase transformations in steels *Steel Res.* **67** 401–7
[5] Shewmon P 1963 *Diffusion in solids series in Materials Science and Engineering* (New York: McGraw-Hill)
[6] Lukas H, Fries S G and Sundman B 2007 *Computational Thermodynamics: The Calphad Method* 1st edn (Cambridge: Cambridge University Press)
[7] Campbell C E, Boettinger W J and Kattner U R 2002 Development of a diffusion mobility database for Ni-base superalloys *Acta Mater.* **50** 775–92
[8] Shang S, Wang Y and kui Liu Z 2010 ESPEI: Extensible, self-optimizing phase equilibrium infrastructure for magnesium alloys *Magnesium Technology 2010 - Held During TMS 2010 Annual Meeting and Exhibition, Magnesium Technology* pp 617–22
[9] Bocklund B, Otis R, Egorov A, Obaied A, Roslyakova I and Liu Z-K 2019 ESPEI for efficient thermodynamic database development, modification, and uncertainty quantification: application to Cu–Mg *MRS Commun.* **9** 618–27
[10] Abrahams K 2020 From atomic mobilities to multi-component interdiffusion simulations in solids: model developmentand automated data assessment *PhD Thesis* Ruhr-Universität Bochum, Bochum, Germany
[11] Borgenstam A, Höglund L, Ågren J and Engström A 2000 DICTRA, a tool for simulation of diffusional transformations in alloys *J. Phase Equilib.* **21** 269
[12] Campbell C E 2008 Assessment of the diffusion mobilites in the γ' and B2 phases in the Ni–Al–Cr system *Acta Mater.* **56** 4277–90
[13] Andersson J O and Ågren J 1992 Models for numerical treatment of multicomponent diffusion in simple phases *J. Appl. Phys.* **72** 1350–5
[14] Jönsson B 1994 Ferromagnetic ordering and diffusion of carbon and nitrogen in bcc Cr–Fe–Ni alloys *Z. Metallkd.* **85** 498–501
[15] Cui Y W, Jiang M, Ohnuma I, Oikawa K, Kainuma R and Ishida K 2008 Computational study of atomic mobility in Co–Fe–Ni ternary fcc alloys *J. Phase Equilib. Diffusion* **29** 312–21
[16] Campbell C E 2005 A new technique for evaluating diffusion mobility parameters *J. Phase Equilib. Diffusion* **26** 435–40
[17] Redlich O and Kister A T 1948 Algebraic representation of thermodynamic properties and the classification of solutions *Ind. Eng. Chem.* **40** 345–8
[18] Kozeschnik E and Buchmayr B 2001 Matcalc–a simulation tool for multicomponent thermodynamics, diffusion and phase transformation kinetics *Mathematical Modelling of Weld Phenomena* 5 (Austria: CRC Press) pp 349–61
[19] Chen J, Liu Y, Sheng G, Lei F and Kang Z 2015 Atomic mobilities, interdiffusivities and their related diffusional behaviors in fcc Co–Cr–Ni alloys *J. Alloys Compd.* **621** 428–33
[20] Dinsdale A T 1991 SGTE data for pure elements *Calphad* **15** 317–425
[21] Interdisciplinary centre for advanced materials simulation (ICAMS) official web-page www.icams.de/content/software-development/. Accessed: 2021-02-08

[22] Zomorodpoosh S, Bocklund B, Obaied A, Otis R, Liu Z-K and Roslyakova I 2020 Statistical approach for automated weighting of datasets: application to heat capacity data *Calphad* **71** 101994
[23] Paulson N H, Zomorodpoosh S, Roslyakova I and Stan M 2020 Comparison of statistically-based methods for automated weighting of experimental data in calphad-type assessment *Calphad* **68** 101728
[24] Hastie T, Tibshirani R and Friedman J 2008 *The Elements of Statistical Learning: Data Mining, Inference, and Prediction Springer Series in Statistics* (Berlin: Springer)
[25] Durrett R 2019 *Probability: Theory and Examples* vol 49 (Cambridge: Cambridge University Press)
[26] Mehrer H 2007 *Diffusion in Solids: Fundamentals, Methods, Materials, Diffusion-Controlled Processes* vol 155 (Berlin: Springer)
[27] Neumann G and Tuijn C 2008 *Self-diffusion and Impurity Diffusion in Pure Metals: Handbook of Experimental Data* vol 14 (Amsterdam: Elsevier)
[28] Tiwari G P and Mehrotra R S 2008 Diffusion and melting *Defect and Diffusion Forum* vol 279 (Switzerland: Trans Tech Publications) pp 23–37
[29] Hargather C Z, Shang S-L, Liu Z-K and Du Y 2014 A first-principles study of self-diffusion coefficients of fcc Ni *Comput. Mater. Sci.* **86** 17–23
[30] Campbell C E, Kattner U R and Liu Z-K 2014 File and data repositories for next generation calphad *Scr. Mater.* **70** 7–11
[31] Otis R A and Liu Z-K 2017 High-throughput thermodynamic modeling and uncertainty quantification for ICME *JOM* **69** 886–92
[32] Duong T C *et al* 2016 Revisiting thermodynamics and kinetic diffusivities of uranium-niobium with Bayesian uncertainty analysis *Calphad* **55** 219–30
[33] Otis R, Bocklund B and Liu Z-K 2020 Sensitivity estimation for calculated phase equilibria *J. Mater. Res.* 1–11
[34] Otis R 2016 Software architecture for CALPHAD modeling of phase stability and transformations in alloy additive manufacturing processes *PhD Thesis* The Pennsylvania State University
[35] Bozdogan H 1987 Model selection and Akaike's information criterion (AIC): the general theory and its analytical extensions *Psychometrika* **52** 345–70
[36] Neumann G and Tuijn C 2008 *Self-diffusion and Impurity Diffusion in Pure Metals: Handbook of Experimental Data* (Amsterdam: Elsevier Science)
[37] Jönsson B 1994 Assessment of the mobilities of Cr, Fe and Ni in fcc Cr–Fe–Ni Alloys *TRITA-MAC-0564*
[38] Jönsson B 1994 Assessment of the mobility of Cr and Fe in fcc Cr–Fe alloys *TRITA-MAC-0563*
[39] Jönsson B 1994 Assessment of the mobility of Cr and Ni in fee Cr–Ni alloys *TRITA-MAC-0562*
[40] Jönsson B 1994 Assessment of the mobility of Fe and Ni in fcc Fe–Ni alloys *TRITA-MAC-0561*
[41] Bakker H *et al* 1990 *Diffusion in Solid Metals and Alloys* vol 26 (Berlin: Springer)
[42] Aucouturier M, De Castro M O P R and Lacombe P 1965 Diffusion du fer radioactif dans le volume et les joints de grains du cobalt, massif ou poreux *Acta Metall.* **13** 125–34
[43] Krishtal M, Mokrov A, Stepanova O and Goncharenko I 1971 *Zashch-Pokryt. Metal* **2** 209
[44] Kuznetsov E 1972 Iron self-diffusion in alloys of the Fe–Ni and Fe–Ni–Cr systems *Uchen. Zap. Gor'kov. Univ.* **148** 38–48
[45] Badia M and Vignes A 1967 Diffusion dans le systeme fer-nickel *Comptes rendus hebdomadaires des seances de l academie des sciences serie* C **264** 18
[46] Lee C G, Iijima Y and Hirano K 1990 Diffusion of chromium in α-iron *Mater. Trans.* **31** 255–61
[47] Badia M and Vignes A 1969 Diffusion du fer, du nickel et du cobalt dans les metaux de transition du groupe du fer *Acta Metall.* **17** 177–87
[48] Lee C G, Iijima Y and Hirano K 1993 Self-diffusion and isotope effect in face-centred cubic cobalt *Defect and Diffusion Forum* vol 95–98 (Trans Tech Publications Ltd) pp 723–8
[49] Bakker H 1968 A curvature in the InD versus 1/T plot for self-diffusion in nickel at temperatures from 980 °C to 1400 °C *Phys. Status Solidi b* **28** 569–76
[50] MacEwan J R, MacEwan J U and Yaffe L 1959 Diffusion of Ni63 in iron, cobalt, nickel, and two iron–nickel alloys *Can. J. Chem.* **37** 1629–36
[51] Maier K, Mehrer H, Lessmann E and Schüle W 1976 Self-diffusion in nickel at low temperatures *Phys. Status Solidi b* **78** 689–98
[52] Bowen A W and Leak G M 1970 Solute diffusion in alpha- and gamma-iron *Metall. Trans.* **1** 1695–700
[53] Mead H W and Birchenall C E 1955 Diffusion of Co60 and Fe55 in cobalt *JOM* **7** 994–5

[54] Bristoti A and Wazzan A 1974 Diffusion of zinc and iron in pure cobalt and diffusion of iron in two iron-cobalt alloys *Rev. Bras. Fis.* **4** 1–10
[55] Million B and Kučera J 1969 Concentration dependence of diffusion of cobalt in nickel–cobalt alloys *Acta Metall.* **17** 339–44
[56] Bronfin M, Bulatov G and Drugova I 1975 Self-diffusion of Ni in the intermetallic compound Ni3Al and pure Ni *Fiz. Met. Metalloved.* **40** 363–6
[57] Million B and Kučera J 1981 Concentration dependence of nickel diffusion in nickel–cobalt alloys *Czech. J. Phys.* **21** 161–71
[58] Buffington F S, Hirano K and Cohen M 1961 Self diffusion in iron *Acta Metall.* **9** 434–9
[59] Million B 1972 Diffusion von Kobalt in Ni–Co–Legierungen bei Temperaturen bis 1000° C *Z. Metallkde.* **63** 484–9
[60] Bussmann W, Herzig C, Rempp W, Maier K and Mehrer H 1979 Isotope effect and self-diffusion in face-centred cubic cobalt *Phys. Status Solidi a* **56** 87–97
[61] Million B, Ržičková J and Vřeštál J 1985 Diffusion in Fe–Ni−Cr alloys with an F.C.C. lattice *Mater. Sci. Eng.* **72** 85–100
[62] Davin A, Leroy V, Coutsouradis D and Habraken L 1963 Comparison of the diffusion of some substitution elements in nickel and cobalt *Cobalt* **19** 51–6
[63] McCoy H J and Murdock J 1963 Influence of argon and hydrogen environments on the rate of diffusion of cobalt-60 in nickel *Am. Soc. Metals Trans. Quart.* **56**
[64] Monma K, Suto H and Oikawa H 1964 Diffusion of Ni63 and Cr51 in nickel–chromium alloys (on the relation between high-temperature creep and diffusion in nickel base solid solutions. I) *J. Japan Inst. Metals Mater.* **28** 188–92
[65] Fedorov G, Smirnov E and Zhomov F 1963 Diffusion and thermodynamic properties of nickel-chromium alloys *Metall. Metalloved. Chistykh* **4** 110–21
[66] Murarka S P, Anand M S and Agarwala R P 1964 Diffusion of chromium in nickel *J. Appl. Phys.* **35** 1339–41
[67] Neiman M, Shinyaev A and Dzantiev B 1955 Diffusion of iron in nickel *Dokl. Akad. Nauk SSSR*
[68] Gaertner D, Kottke J, Wilde G, Divinski S V and Chumlyakov Y 2018 Tracer diffusion in single crystalline Co–Cr–Fe–Ni and Co–Cr–Fe–Mn–Ni high entropy alloys *J. Mater. Res.* **33** 3184–91
[69] Neiman M and Shinyaev A 1955 Investigation of iron diffusion in iron–nickel alloys *Dokl. Akad. Nauk SSSR* **102** 969–72
[70] Gruzin P 1954 Diffusion of cobalt, chromium, and tungsten in iron and steel *Dok. Akad. Nauk SSSR* **94** 681–4
[71] Neumann G and Tölle V 1986 Monovacancy and divacancy contributions to self-diffusion in face-centred cubic metals reanalysis for copper, silver, gold, nickel and platinum *Phil. Mag.* A **54** 619–29
[72] Gruzin P and Fedorov G 1955 The diffusion of chromium in the nickel base solid solutions *Doklady Akad. Nauk SSSR* **105** 264–7
[73] Neumann G, Tölle V and Tuijn C 2001 Application of the modified electrostatic model to the impurity diffusion in cobalt *Physica* B **304** 298–303
[74] Guiraldenq P 1962 Comparison of volume and grain-boundary self-diffusion phenomena in sintered and solid iron *C.R. Acad. Sci.* **254** 99–101
[75] Nix F C and Jaumot F E 1951 Self-diffusion in cobalt *Phys. Rev.* **82** 72–4
[76] Hässner A and Lange W 1965 Volumenselbstdiffusion in kobalt–nickel–legierungen *Phys. Status solidi b* **8** 77–91
[77] Nohara K and Hirano K 1970 Diffusion of manganese into iron *Proc. Int. Conf. on Science Technology of Iron Steel* vol 7
[78] Henry G, Barreau G and Cizeron G 1975 Coefficients of volume diffusion of Co in gamma Fe and in Fe–Co alloys *C R Acad. Sci.* **280** 1007–10
[79] Nohara K and Hirano K 1971 Diffusion of Mn in Fe and Fe–Mn alloys *Suppl. Trans. Iron Steel Japan* **11** 1267–73
[80] Henry G and Cizeron G 1978 Diffusion of nickel into FCC iron–nickel alloys-comparison with other results related to diffusion into FCC solid *Ann. Chim. France* **3** 167–76
[81] Nohara K and Hirano K-i 1973 Self-diffusion and interdiffusion in γ solid solutions of the Fe–Mn systems *J. Japan Inst. Metals Mater.* **37** 51–61
[82] Heumann T and Imm R 1968 Self-diffusion and isotope effect in γ-iron *J. Phys. Chem. Solids* **29** 1613–21
[83] De Reca E W and Pampillo C 1967 Self-diffusion of Ni in Ni–Fe alloys *Acta Metall.* **15** 1263–8

[84] Hirano K i, Agarwala R P, Averbach B L and Cohen M 1962 Diffusion in cobalt-nickel alloys *J. Appl. Phys.* **33** 3049–54
[85] Rothman S J, Nowicki L J and Murch G E 1980 Self-diffusion in austenitic Fe–C–Ni alloys *J. Phys. F: Met. Phys.* **10** 383–98
[86] Hirano K-i and Cohen M 1972 Diffusion of cobalt in iron–cobalt alloys *Trans. Japan Inst. Metals* **13** 96–102
[87] Ržičková J and Million B 1981 Self-diffusion of the components in the F.C.C. phase of binary solid solutions of the Fe–Ni–Cr system *Mater. Sci. Eng.* **50** 59–64
[88] Hoffman R, Pikus F and Ward R 1956 Self-diffusion in solid nickel *J. Metals* **8**
[89] Huntz A 1973 Influence of the chrome content and the interstitial impurities content/carbon and nitrogen/on the volumetric and intergranular diffusion of iron 59* in iron *Mem. Sci. Rev. Met.* **70**
[90] Shinyayev A. Y. 1963 *Fiz. Met. Metalloved.* **15** 100–4
[91] Iijima Y, Hirano K-I and Taguchi O 1977 Diffusion of manganese in cobalt and cobalt–manganese alloys *Phil. Mag.* **35** 229–44
[92] Suzuoka T 1961 Lattice diffusion and grain boundary diffusion of cobalt in γ-iron *Trans. Japan Inst. Metals* **2** 176–81
[93] Ivantsov I 1966 Self-diffusion in monocrystalline nickel *Fiz. Met. Metalloved.* **22** 5
[94] Swalin R and Martin A 1956 Solute diffusion in nickel-base substitutional solid solutions *J. Metals* **8**
[95] Jung S B, Yamane T, Minamino Y, Hirao K, Araki H and Saji S 1992 Interdiffusion and its size effect in nickel solid solutions of Ni–Co, Ni–Cr and Ni–Ti systems *J. Mater. Sci. Lett.* **11** 1333–7
[96] Vladimirov A, Kajgorodov V, Klotsman S and Trakhtenberg I 1978 Volume diffusion of cobalt and tungsten in nickel *Fiz. Met. Metalloved.* **46** 1232–9
[97] Kohn A, Levasseur J, Philibert J and Wanin M 1970 Essai de verification experimentale des theories de l'effet kirkendall dans les systemes fer–nickel et fer–cobalt *Acta Metall.* **18** 163–73
[98] Wazzan A R 1965 Lattice and grain boundary self-diffusion in nickel *J. Appl. Phys.* **36** 3596–9